Biomedical Microdevices 2:3, 169–174, 2000


# *Focused Flow Micropump Using Ultrasonic Flexural Plate Waves*

*Audra H. Meng, Nam-Trung Nguyen, and Richard M. White*

*Berkeley Sensor & Actuator Center, Department of Electrical Engineering and Computer Science University of California, Berkeley, CA 94720*

*Abstract.* **In this paper, a micromachined pump is presented that uses ultrasonic flexural plate waves traveling along a thin membrane to excite an acoustic field in the fluid that is in contact with the membrane. The acoustic field generates fluid flow by the mechanism of acoustic streaming. A novel combination of radial transducers and unidirectional fluid flow produces a fluid micropump capable of achieving flow speeds up to 1.15 millimeters per second, much faster than flow speeds previously obtained. In addition, the radial transducers successfully focused 2-micron polystyrene spheres over a beam waist of less than 100 microns. Also presented are techniques used to characterize thipt>**

*Key Words.* **ultrasonic, flexural, focused, microfluidic, micromachine**

## 1. Introduction

The quest for practical, inexpensive micromachined flow systems plays a critical role in the realization of small-scale chemical analysis systems. Many different approaches for micropumping exist [1], including piezoelectrically [2] and electrostatically [3] actuated diaphragm pumps, as well as electrophoretic [4], electrohydrodynamic [5,6], and thermal bubble pumps [7,8]. This paper presents an acoustically driven micropump which offers the advantages of low operating voltages, gentle pumping with no valves or heating involved, and no limitations on the type of liquid or gas that can be pumped. The micropump discussed here represents a continuation of previous work [9,10], with a novel transducer geometry resulting in faster pumping speeds and improved focusing ability.

The classical flexural plate-wave device, shown in Figure 1, consists of a thin silicon nitride membrane with aluminum and piezoelectric zinc oxide transducers patterned on the membrane [11–13]. These interdigitated transducers launch acoustic plate waves that travel along the membrane, producing an acoustic field that can be used to pump liquids or gases by the mechanism of acoustic streaming [14,15]. Other applications of the flexural plate-wave device includes liquid density and viscosity sensing [16,17], as well as mixing for increased chemical reaction rates [18].

The pumping mechanism is gentle and was shown to safely pump DNA 4,400 base pairs in length suspended in a liquid with wave amplitudes up to tens of nanometers without causing strand breakage [19]. For this reason, this system can be used to pump liquids containing DNA and other biological samples of interest. Possible applications of this technology include sample transport in miniature chemical analysis systems as well as pumping for microfabricated cell counters, cell sorting, or drug delivery systems.

## 2. Fabrication and Design

### 2.1. Device fabrication

Using LPCVD, low-stress silicon nitride (1-micron thick) is deposited on a $\langle 100 \rangle$ silicon wafer. On the back side of the wafer, windows for forming the well are patterned and opened in the nitride by plasma etching. Next, the wafer is placed into KOH solution for bulk etching of the silicon from the back side. Once the membranes have been formed, aluminum (0.25-microns thick) is sputtered on the front side of the wafer and the interdigitated transducers are patterned. A thin layer of low temperature oxide is deposited on the wafer before the piezoelectric zinc oxide (1.5-microns thick) is RF-magnetron sputtered onto the front side of the wafer. More aluminum is deposited and patterned to form the ground plane. Finally, the zinc oxide film is etched to expose the transducer contacts underneath. A detailed description of the process flow can be found in [11].

### 2.2. Unidirectional flow

The pump produces unidirectional flow using a transducer design technique developed by Bradley [10]. In the standard bidirectional flexural plate-wave device, two sets of transducer fingers are interdigitated and spaced so that the fingers are half a wavelength apart

Contact author: Audra Meng, Berkeley Sensor & Actuator Center, 497 Cory Hall, University of California, Berkeley, CA 94720, E-mail: ameng@bsac.eecs.berkeley.edu

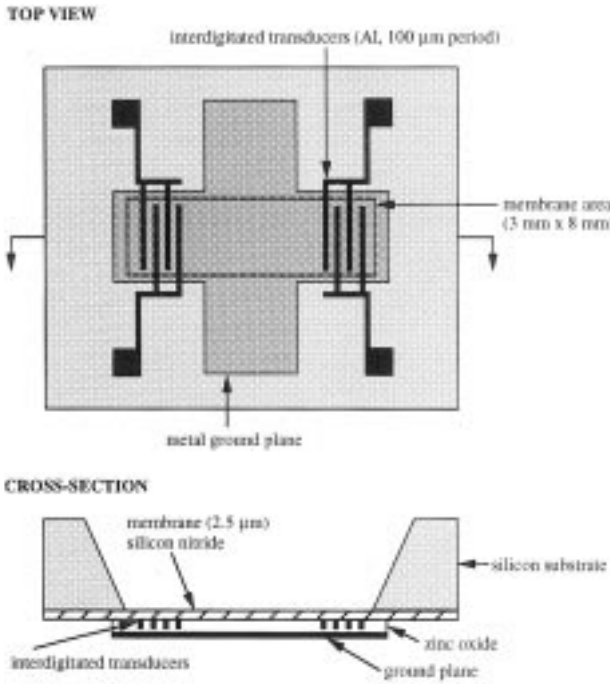


***Fig. 1.*** *The classical flexural plate-wave device. The top view of the device is diagrammatic and shows the placement of all overlapping layers. The cross-sectional view shows the layers in correct order, with the vertical axis expanded for clarity. The device illustrated has a well volume of about 12 microliters.*

(center-to-center). A voltage source connected between the transducer fingers and the underlying ground plane drives one half of a set of fingers, and its phase-inverted complement drives the other half. The flexural plate waves launched by these sets of transducers add constructively in both directions, giving bidirectional transduction as indicated in Figure 2.

For this device, each transducer finger pair is spaced one quarter wavelength apart. This transducer finger pair pattern is repeated at wavelength intervals to give the quadrature unidirectional interdigitated transducers, which are also illustrated in Figure 2. One set of fingers is driven by a signal, and the other set of fingers is driven by a signal which is 90 degrees out of phase with the first. Now, the flexural plate waves that are launched add constructively in one direction while combining destructively in the other. In this way, unidirectional transduction is achieved.

### *2.3. Radial transducers*

The micropump was designed to focus ultrasonic energy to a beam waist of approximately 100 microns using the Gaussian beam focusing of flexural plate waves first demonstrated by Moroney [9]. By making the interdigitated transducers circular instead of linear, as shown

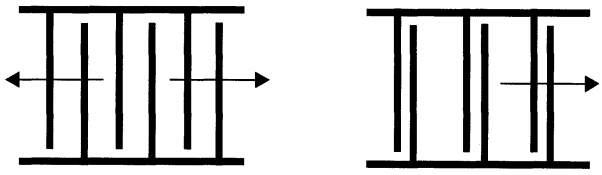

***Fig. 2.*** *Bidirectional and unidirectional transducers.*

in Figure 3, the acoustical energy is focused in a way that can be described by Gaussian beam theory. The Gaussian mode solution for flexural waves in a thin membrane can be characterized by three functions, the beam waist $w(x)$, the wavefront radius of curvature $R(x)$, and the on-axis phase $\eta(x,t)$.

$$w^2(x) = w_0^2\left[1 + \left(\frac{\lambda x}{\pi w_0^2}\right)^2\right], \tag{1}$$

$$R(x) = x\left[1 + \left(\frac{\pi w_0^2}{\lambda x}\right)^2\right], \tag{2}$$

$$\eta(x,t) = \eta_0 + \frac{2\pi x}{\lambda} - \omega t - \arctan\left(\frac{\lambda x}{\pi w_0^2}\right), \tag{3}$$

where $w_0$ is the beam waist at the focus, $x = 0$. The beam divergence angle is calculated from equation (1) using the relation $\tan\theta = dw(x)/dx$ for large $x$. From this we have

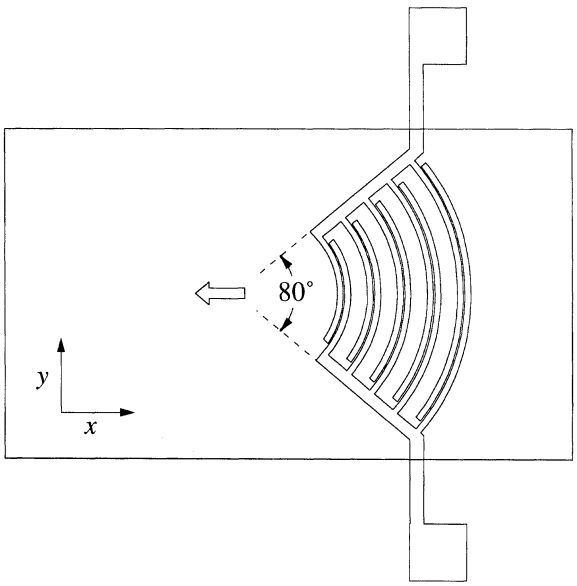


***Fig. 3.*** *Top view of radial transducers, spaced in a λ/4, 3λ/4 arrangement for unidirectional pumping. The large arrow indicates the pumping direction.*

$$w_0 = \frac{\lambda}{\pi \tan \theta} \tag{4}$$

The beam depth of focus $x_0$, defined as the distance from focus where $w = 2w_0$ is also calculated from equation (1)

$$x_0 = \frac{\pi w_0^2}{\lambda} = \frac{\lambda}{\pi \tan^2 \theta} \tag{5}$$

The boundary of the Gaussian beam near the focus is shown in Figure 4. For this device, an angle of $\theta = 40^\circ$ was chosen so that the transducers subtend an angle of $80^\circ$ as viewed from the focal point. The wavelength of the device (determined by the transducer period) is 100 microns and there are a total of 15 transducer finger pairs, each finger measuring 20 microns in width. The predicted beam waist $w_0$ and depth of focus $x_0$ are 38 and 45 microns, respectively. By focusing the acoustic energy in this manner, the device is able to produce large amplitude waves which in turn generate large streaming velocities.

### *2.4. Simulation of the acoustic theory*

It may be expected that the unidirectional radial transducers on the device would result in the focused pumping of liquids. To test this idea, a quantitative model of the fluid flow on the membrane was constructed. Numerical simulations were performed using a commercial computational fluid dynamics software package (CFD Research Corporation). The CFD code solves the continuity equation, the momentum equation, and the energy equation [20,21]. The software permits the user to modify the fluid density using the ideal gas law or a second-order function of pressure. Furthermore, the temperature dependency of fluid properties can be considered. Results presented here will neglect the temperature dependency.

Figure 5 describes the 3-dimensional model of the membrane of the focused flow pump. A user library routine written in FORTRAN modifies the grid positions.

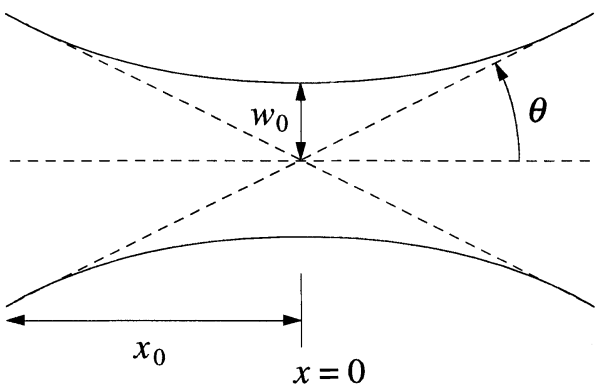


***Fig. 4.*** *The Gaussian beam near the focus.*

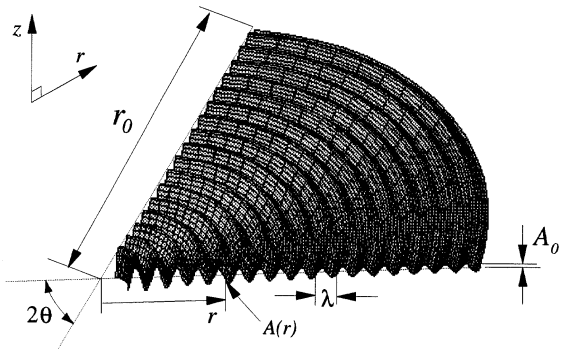


***Fig. 5.*** *Model of the flexural plate wave membrane. The radial coordinate is r (outer edge of transducers is at $r_0$), $A(r)$ is the wave amplitude (starting at $A_0$ at the outer edge), θ is the convergence angle, and the z axis is normal to the membrane.*

The vertical displacement, $\Delta z$, and the radial displacement, $\Delta r$, of the device are given by [22].

$$\begin{aligned} \Delta z &= A(r,t)\sin(\omega t - kr) \\ \Delta r &= (A(r,t)\pi d/\lambda)\cos(\omega t - kx), \end{aligned} \tag{6}$$

where $A$ is the wave amplitude, $\omega = 2\pi f$ is the angular frequency of the wave, $k = 2\pi/\lambda$ is the wave number, and $d$ is the membrane thickness. The displacement along the direction orthogonal to $z$ and $r$ is neglected. The wave amplitude is given by [23].

$$A = \frac{1}{\omega}\sqrt{\frac{2P_{\text{avg}}}{M_\rho w v_\text{p}}}, \tag{7}$$

where $P_{\text{avg}}$ is the time-averaged acoustic power flowing in the wave, $M_\rho$ is the areal mass density of the plate, $w$ is the width of the acoustic beam, and $v_\text{p}$ is the phase velocity of the flexural plate wave. Since the acoustic beam width is proportional to the radius,

$$w = 2\theta r, \tag{8}$$

where θ is the convergence angle, energy conservation requires the wave amplitude to have the form

$$A(r) = A_0\sqrt{\frac{r_0}{r}}, \tag{9}$$

where $A_0$ and $r_0$ are constants. We model the buildup of the wave in time by assuming the functional form

$$A(r,t) = A_0\sqrt{\frac{r_0}{r}}(1 - \exp(-t/\tau)), \tag{10}$$

where τ is a time constant for the wave buildup, assumed here to be the wave period ($\tau = 1/f$). Figure 6 illustrates the time-averaged velocity field of the pump, and Figure 7 indicates the variation of flow velocity with distance

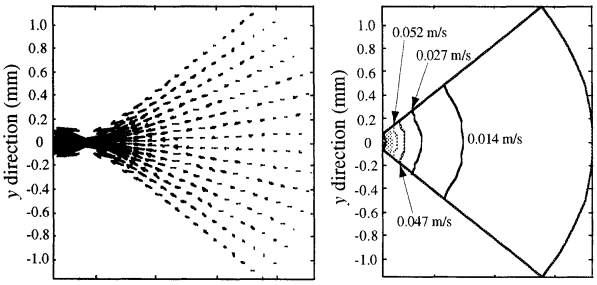


*Fig. 6. Simulation results for the time-averaged velocity field in the focused flow pump, showing increasing flow velocity as the focal point is approached.*

above the membrane. It is seen that the focused pumping of liquid does occur next to the membrane, within a layer approximately 20 microns thick.

## 3. Experimental Results

### 3.1. Focusing and flow velocities

Devices have been tested and were found to successfully focus the flow of 2-micron diameter polystyrene spheres (specific gravity 1.05) in water. Pumping velocities were significantly greater in the beam waist region, with observed pumping speeds of over 1 millimeter per second.

For testing, the well side of the device was filled with water containing polystyrene spheres using a micropipette. Approximately 20 microliters of liquid was used to over-fill the well, and a glass coverslip was placed over the top of the well giving a channel depth of 500 microns (the thickness of the silicon wafer). Video recordings of the pumping were made looking down at the device through the glass coverslip with an optical microscope using a 40 × objective. Afterwards, the videotape was analyzed frame by frame to determine pumping velocities. The microscope was focused on the spheres that were closest to the driven membrane, where the fastest flow speeds occur.

Using an input voltage of 12 volts (zero to peak) at the device resonant frequency of 3.79 MHz, the maximum measured flow velocity was approximately 1.15 millimeters per second. Higher velocities were observed, but the values could not be measured. The flow velocity in the beam waist region was so high that the spheres appear blurred on the videotape. Since only the slower spheres could be resolved, this observed flow velocity was not the maximum velocity achieved.

### 3.2. Flow analysis

Particle image velocimetry (PIV) was used to analyze the focus flow micropump. This technique measures the displacement of the image of a particle on two or more successive frames of video taken $\frac{1}{30}$th of a second apart. Using a CCD camera attached to an optical microscope, video images of the fluid flow were taken. A standard VCR was used to record the data, and sequential images were used for the PIV analysis. Velocity field results from the PIV analysis are shown in Figure 8. The solid curve is a fit of the flow velocity to the functional form $v = a/(r - b)$, where $r$ is the radial distance from the focal point and $a$ and $b$ are fit parameters. This form is expected from the relations $v \propto A^2$ and equation (9). The coefficient $b$ is included to account for any experimental error in the assumed position of the focal point. It is seen that the Gaussian beam model describes the scaling of the flow velocity near the focal point quite well.

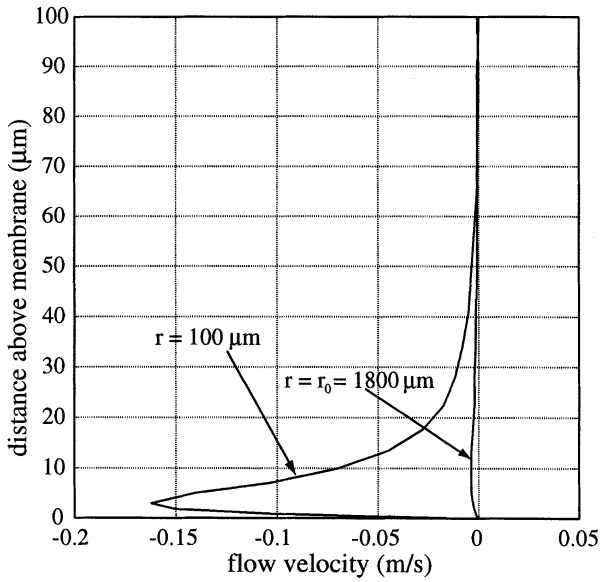


*Fig. 7. Calculated flow velocity as a function of distance above the membrane, near the focal point and at the outer edge of the transducer* $(r = r_0)$.

### 3.3. Laser diffraction measurements

A scanning laser diffraction system was developed to measure the displacement amplitude of the membrane. This system consisted of an $xy$-translation stage with actuators connected to a programmable controller (Newport Corp). A Macintosh computer running LabVIEW was used to operate the controller and acquire data. By mounting the focused flow device onto the translation stage, the surface of the membrane could be scanned in both the $x$ and $y$ directions. A LabVIEW program was written to automate the process of scanning the membrane in a serpentine fashion, with step sizes specified by the user.

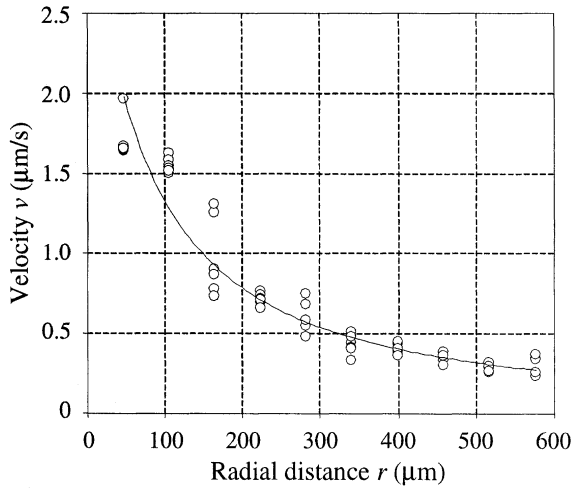


***Fig. 8.*** *Flow velocity as a function of distance, r, from focus, measured using the PIV technique. The pumping speed was substantially slowed to allow image acquisition using a standard NTSC video-rate camera. The solid curve fits the data to the form expected from the Gaussian beam model.*

An accurate method of measuring the spatial amplitude of the membrane wave motion is to look for diffraction in a laser beam reflected from the driven membrane surface. When the diameter of the laser beam is larger than the wavelength of the device, a diffraction pattern results. The maximum plate wave amplitude $A$ can be calculated from the intensity of the first diffracted order

$$A = \frac{\lambda_{op}}{2\pi \cos \phi} \sqrt{\frac{I_1}{I_{inc}}}, \tag{11}$$

where $\lambda_{op}$ is the optical wavelength, $\phi$ is the angle of incidence relative to the normal between the optical path and acoustic path, $I_1$ is the intensity of the first diffracted order, and $I_{inc}$ is the intensity of the incident light. A HeNe laser with a wavelength of 632.8 nanometers was used, and a photodetector was used to measure the intensity of the first diffracted order and the incident light.

A thin layer of aluminum (250 nanometers) was deposited over the entire surface inside the well of the device to serve as a reflective surface for the laser beam. A series of mirrors were used to direct the laser beam to the surface of the device, and the reflected light from the membrane to the photodetector. In addition, a lens was added to focus the 1.5 millimeter diameter laser beam down to approximately 500 microns in diameter, allowing higher resolution data to be obtained. The setup is shown in Figure 9.

Figure 10 shows the results of the scanning laser

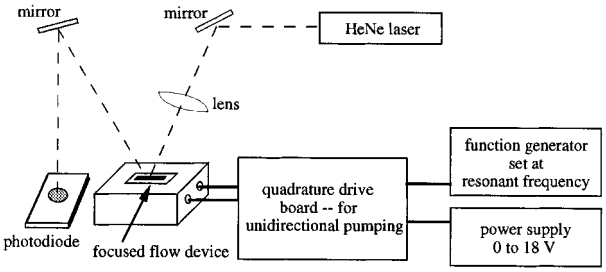


***Fig. 9.*** *Laser diffraction experimental setup.*

diffraction measurement on the focused flow device. The wave amplitude was not measured over the transducer area because the aluminum transducers scattered light from the laser, interfering with the diffraction pattern. The wave amplitude (in nanometers) is plotted versus position on the device surface. From these results, the focusing ability of the device predicted earlier by Gaussian beam theory can be clearly observed.

## 4. *Discussion and Conclusion*

This paper presents a micromachined acoustic pump that uses a novel combination of radial transducers and unidirectional fluid flow to produce focused pumping with flow speeds up to 1.15 millimeters per second. The radial transducers successfully focused 2-micron polystyrene spheres over a beam waist of less than 100 microns. Also presented are simulation techniques and experimental methods used to characterize this

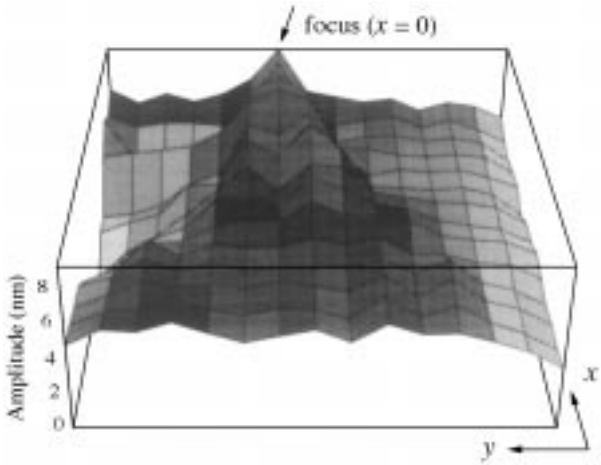


***Fig. 10.*** *Measured wave amplitude over a square region of the membrane 2 millimeters on a side. The wave focus is shown at the top, with unidirectional flow fanning out in a downward direction. The transducers, not shown here, would lie above the focal point at the top of the figure.*

micropump. These analysis techniques can be useful tools for the design optimization of micropumps such as the one presented here. This acoustically driven micropump offers the advantages of low operating voltages, gentle pumping with no valves or heating involved, and no limitations on the type of liquid or gas that can be pumped. Possible applications of this technology include sample transport in miniature chemical analysis systems, and pumping for microfabricated cell counters cell sorting, or drug delivery systems.

## *Acknowledgments*

Devices were fabricated in the Berkeley Microfabrication Laboratory. The authors would like to thank Amy Wang for sharing her knowledge and insight on the fabrication process.

## *References*

1. P. Gravesen, J. Branebjerg, and O.S. Jensen, J. Micromech. Microeng. **3**, 168 (1993).
2. V. Gass, B.H. Van Der Schoot, S. Jeanneret, and N.F. De Rooij, *Tech. Digest IEEE Transducers* (Yokohama, 1993), p. 1048.
3. R. Zengerle, M. Richter, F. Brosmger, A. Richter, and H. Sandmaier, *Tech. Digest IEEE Transducers* (Yokohama, 1993), p. 106.
4. A. Manz, D.J. Harrison, J.C. Fettinger, E. Verpoorten, H. Ludi, and H.M. Widmer, *Tech. Digest IEEE Transducers* (San Francisco, CA, 1991), p. 939.
5. A. Richter, H. Sandmaier, and A. Plettner, *Proc. Micro System Technologies 90* (Berlin, 1990), p. 812.
6. G. Fuhr, R. Hagedorn, T. Muller, W. Benecke, and B. Wagner, *Proc. Micro Electro Mechanical Systems* (Travemunde, Germany, 1992), p. 25.
7. L. Lin, A.P. Pisano, and A.P. Lee, *Tech. Digest IEEE Transducers* (San Francisco, CA, 1991), p. 1041.
8. J. Evans, D. Liepmann, and A.P. Pisano, *Proc. Micro Electro Mechanical Systems* (Nagoya, Japan, 1997), p. 96.
9. R.M. Moroney, R.M. White, and R.T. Howe, ASME Winter Annual Meeting **DSC-32**, 181 (1991).
10. C.E. Bradley, J.M. Bustillo, and R.M. White, IEEE Ultrasonics Symposium **1**, 505 (1995).
11. S.W. Wenzel and R.M. White, IEEE Trans. Electron Devices **ED-35**, 735 (1988).
12. J.W. Grate, S.W. Wenzel, and R.M. White, Analytical Chemistry **63**, 1552 (1991).
13. D.S. Ballantine, R.M. White, S.J. Martin, A.J. Ricco, E.T. Zellers, G.C. Frye, and H. Wohltjen, *Acoustic Wave Sensors Theory, Design, and Physico-Chemical Applications* (Academic Press, San Diego, 1997), p. 111.
14. R.M. Moroney, R.M. White, and R.T. Howe, Applied Physics Letters **59**, 774 (1991).
15. P. Luginbuhl, S.D. Collins, G.-A. Racine, and M.-A. Gretillat et al., Journal of Microelectromechanical Systems **6**, 337 (1997).
16. B.A. Martin, S.W. Wenzel, and R.M. White, Sensors and Actuators **A21–A23**, 704 (1990).
17. T.K. Eto, B.J. Costello, S.W. Wenzel, R.M. White, and B.J. Rubinsky, Journal of Biomechanical Engineering **115**, 329 (1993).
18. T.R. Tsao, R.M. Moroney, B.A. Martin, and R.M. White, Proc. IEEE Ultrasonics Symposium **2**, 937 (1991).
19. A.H. Meng and R.M. White, Micro- and Nanofabricated Electro-Optical Mechanical Systems for Biomedical and Environmental Applications **2978**, 227 (1997).
20. N.T. Nguyen, R.G. Doering, and R.M. White, Supplement Digest, Hilton Head Workshop, Hilton Head, 31 (1998).
21. N.T. Nguyen, R.G. Doering, A. Lal, and R.M. White, *IEEE International Ultrasonics Symposium* (Sendai, Japan, 1998).
22. T. Sashida and T. Kenjio, *An Introduction to Ultrasonic Motors*, (Clarendon Press, Oxford, 1993), p. 130.
23. R.M. Moroney, *Ultrasonic Microtransport, PhD Thesis, EECS Department* (University of California, Berkeley, 1995), p. 17.